

# TERAHERTZ-DRIVEN MeV ELECTRON BUNCH COMPRESSION AND STREAKING \*

Y. Xu, Y. Song, J. Wang, C. Tsai, K. Fan<sup>†</sup>, Z. Liu<sup>‡</sup>, School of Electric and Electronic Engineering, Huazhong University of Science and Technology, Wuhan, China

## Abstract

Electron bunches with ultra-short bunch length and ultra-high timing stability are crucial for various applications. To achieve these desired characteristics, there is a growing interest in employing Terahertz-driven techniques to manipulate and diagnose electron bunches. This paper presents a method capable of compressing and measuring electron bunch lengths. Theoretical and simulation results demonstrate that the bunch length of 54 fs is reduced to 4 fs by utilizing THz-driven resonant cavity compression, achieving a compression ratio of 13. Furthermore, we also verify the bunch compression using a terahertz-driven streak camera.

## INTRODUCTION

Ultra-short and precisely timed electron bunches are essential for applications such as ultrafast electron diffraction (UED) and free-electron lasers (FELs) [1-3]. In UED, the temporal resolution relies on the quality of the electron bunch used as a probe. Both the bunch length and the timing jitter relative to the laser can impact the overall system resolution. RF deflecting cavities are commonly employed to compress the bunch length while maintaining low emittance [4-5]. However, the phase jitter of the RF resonant field introduces energy instability to the electron bunch, resulting in a time-of-arrival (TOA) jitter typically ranging from tens to hundreds of femtoseconds. THz-driven bunch manipulation enables the generation of electron bunches with femtosecond-scale lengths and high-timing stability.

This all-optical method ensures inherent synchronization between the THz field and the electron bunch, enabling precise manipulation without inducing time jitter [6]. Various demonstrations of THz-driven techniques have been reported. For example, butterfly-shaped resonators compress and diagnose keV-level electron bunches [7], and parallel-plate waveguide structures compress MeV-level electron bunches [8]. The segmented terahertz electron accelerator and manipulator (STEAM) structure offers a multifunctional design for compression and measurement [9]. These studies highlight the potential of strong-field THz techniques for manipulating and diagnosing electron bunches.

This paper presents a method illustrated in Fig. 1 to compress and diagnose electron bunches using THz-driven resonators. A buncher generates a longitudinally polarized field for compressing the electron bunch length, while a slit downstream serves as a THz-driven streak camera to measure the bunch length. Despite the space charge effect

causing continuous expansion in both longitudinal and transverse directions, passing the electron bunch through the THz electric field at the zero-crossing phase achieves opposite momenta for the head and tail electrons, resulting in the minimum bunch length at the sample position. At this position, a transversely polarized THz field generated by the slit converts the electron bunch's longitudinal temporal information into a transverse bunch distribution. Analyzing the measurements from the detector allows us to infer the bunch length and time of arrival. The effectiveness has been verified through theoretical analysis and numerical simulations, demonstrating its capability to compress and evaluate MeV-level electron bunches.

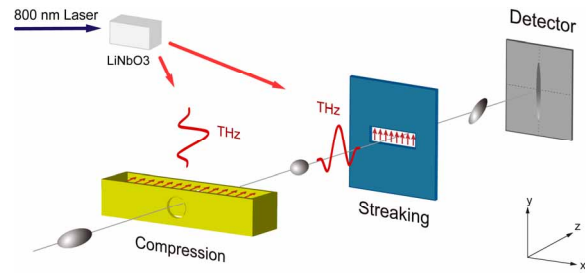


Figure 1: Schematic of the compression and streaking system.

## THz-DRIVEN ELECTRON BUNCH COMPRESSION

Figure 2 illustrates the THz buncher structure along with its equivalent LC circuit model, which can be simplified as a resonator. The driving THz driving pulse, polarized along the z-axis, enters the buncher from the top. As a result of resonance, an enhanced THz field is generated in the gap, with the amplitude and frequency dependent on both the driving THz pulse and the buncher geometric parameters. The THz electric field mainly concentrates near the channel through which the electron beam passes and has a uniform amplitude, as shown in Fig. 2 (b).

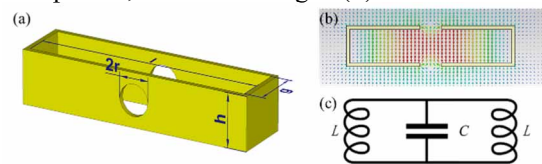


Figure 2: (a) The structure of the THz buncher. (b) The electric field distribution in buncher. (c) The equivalent LC circuit of the buncher.

Due to the structural symmetry, the gap exhibits a strong electric field while having an almost negligible magnetic field. These characteristics make the buncher well-suited for beam compression. When an electron beam passes

\* Work supported by NSFC 12235005 and the State Grid Corporation of China Technology Project 5400-202199556A-0-5-ZN

<sup>†</sup>kjfan@hust.edu.cn, <sup>‡</sup>zzliu@hust.edu.cn

through the buncher, the longitudinal THz electric field will compress the electron beam, reducing its size and duration.

Table 1: Dimensions of the Buncher

Dimensions	Value ( $\mu\text{m}$ )
$l$	454
$h$	100
$g$	100
$r$	30

The structure of the buncher can be described by four parameters, as illustrated in Fig. 2 (a) and Table 1. The resonant frequency of the THz field in the gap can be approximated using an LC resonant circuit, as depicted in Fig. 2 (c). In this circuit model, the planes on either side of the circular aperture are regarded as a parallel-plate capacitor, while the conductor carrying the electron flow is treated as an inductor. Hence, the resonant frequency of the buncher can be calculated using the following expression:

$$f_0 = \frac{c}{s} = \frac{c}{2(l+g)-4r} \quad (1)$$

Here,  $c$  is the speed of light, which represents the propagation velocity of the current in the conductor. Similarly, the distance the current travels in one loop  $s$  can be approximated as the circumference of the inner diameter of the buncher. The parameters ( $l$ ) and ( $g$ ) are the key factors in optimizing the buncher resonant frequency. These parameters primarily control the resonant behavior of the system. Meanwhile, the parameter ( $h$ ) has minimal influence on the charge density distribution around the circular apertures and can be disregarded.

The compression efficiency of the buncher is primarily influenced by two factors: the THz electric field amplitude and the transit time of the electron bunch. Increasing the parameter  $g$  extends the interaction time between the electric field and the electron bunch, thereby improving the compression efficiency. However, it's important to note that increasing  $g$  also leads to drawbacks, including higher radiation power of the THz field, rapid energy decay of the electric field, and a decrease in the quality factor of the buncher. Therefore, when designing a buncher, it is crucial to consider the specific application scenario and strike a balance between compression efficiency and the aforementioned trade-offs.

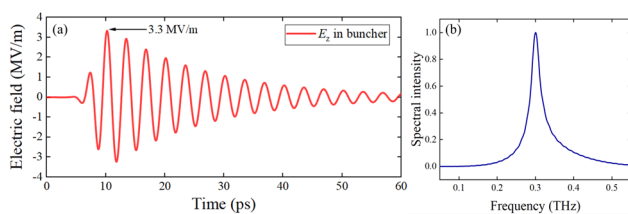


Figure 3: (a) The electric fields at the center of the buncher. (b) The corresponding spectrum.

To generate a larger amplitude THz field, we use a quasi-Gaussian single-pulse THz wave with a central frequency of 0.3 THz, which closely matches the resonance

frequency of the buncher, allowing for effective excitation. CST simulations indicate that the buncher can enhance the THz electric field by a factor of 3.3. The waveform and spectrum are shown in Fig. 3. When the longitudinal center of the beam aligns with the zero-crossing phase of the THz field, two distinct effects occur. The electrons at the head of the beam experience deceleration, while those at the tail experience acceleration. As a result, the overall bunch length decrease after a drift section.

This beam compression dynamics process can be described using a transfer matrix. The coordinates of an individual electron in the longitudinal phase space are defined as  $(\zeta_0, \delta_0)$ , where  $\zeta$  represents the relative position of the electron with respect to the beam center, and  $\delta$  represents the relative energy difference to the reference particle. The coordinates  $(\zeta_1, \delta_1)$  of the electron in the longitudinal phase space after passing through the THz buncher can be described by the following equation:

$$\begin{bmatrix} \zeta_1 \\ \delta_1 \end{bmatrix} = \begin{bmatrix} 1 & L/\beta^2\gamma^2 \\ 0 & 1 \end{bmatrix} \begin{bmatrix} 1 & 0 \\ -k\Delta V/E_{\text{ref}} & 1 \end{bmatrix} \begin{bmatrix} \zeta_0 \\ \delta_0 \end{bmatrix} \quad (2)$$

Here,  $L/\beta^2\gamma^2$  is the momentum compression factor of the drift section,  $k = 2\pi f_0/\beta c$  is the wave number of the THz field,  $E_{\text{ref}}$  is the energy of the electron beam, and  $\Delta V$  is the effective voltage of the THz resonator.

Given a specific THz electric field amplitude, this equation allows us to determine the position where the bunch length is minimized after compression. It is important to highlight that the theoretical model does not account for the space charge effect. Additionally, the buncher is limited to compensate for the linear bunch chirp of the electron beam. Further studies are needed for beams dominated by space charge to address and compensate for the space-charge effect.

## THZ-DRIVEN STREAK CAMERA

The electron beam passes through the buncher, where it undergoes compression to achieve its shortest length at the sample location. A deflection cavity is placed at that location to measure the size of this compressed beam. The slit used for beam length measurement is depicted in Fig. 4 (a), and its geometric parameters are shown in Table 2.

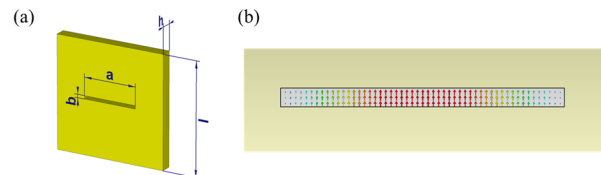


Figure 4: (a) The structure of the slit. (b) The electric field distribution in the slit.

The same slit is also excited by the aforementioned driving THz pulse, with the polarization direction along the  $y$ -axis. Fig. 4 (b) illustrates the electric field distribution generated within the slit gap. Horizontally, the strongest electric field is concentrated in the center, while it gradually weakens towards the sides. In the case of electron bunches with small transverse sizes, the electric field exhibits uniformity.

Table 2: Dimensions of the Slit

Dimensions	Value ( $\mu\text{m}$ )
$l$	2000
$b$	30
$a$	480
$h$	100

Figure 5 presents the waveform and spectrum of the THz electric field at the center of the rectangular slit. The field exhibits an enhancement factor of 7.0. In this slit resonator, the enhancement factor of the generated field is primarily influenced by the width of the slit. A narrower slit corresponds to a higher enhancement factor. Theoretical analysis indicates that the enhancement factor can be approximated as the ratio of the longer side to the shorter side of the slit.

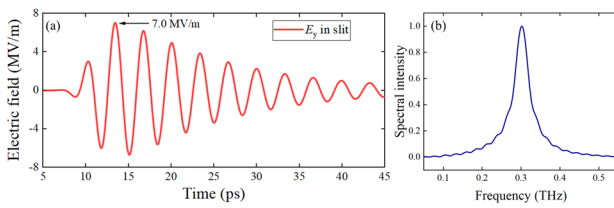


Figure 5: (a) The electric fields at the center of the slit. (b) The corresponding spectrum.

When the electron bunch passes through the THz electric field at the zero-crossing phase, it acquires a net transverse momentum of zero. Although the direction of the bunch motion remains unchanged, the leading and trailing electrons acquire transverse momenta in opposite directions. After a drift section, the longitudinal characteristics of the bunch are transformed into a transverse distribution on the detector. The bunch length can be deduced by utilizing the following formula, which relates it to the transverse size:

$$S = \frac{2e\bar{E}_y}{\sqrt{3}P} \sin\left(\frac{\omega}{2} T_p\right) D\Delta T \quad (3)$$

where  $\omega$  is the angular frequency of the deflecting electric field,  $\bar{E}_y$  is the effective deflecting field strength,  $e$  is the elementary charge,  $P$  is the momentum of the electron bunch,  $D$  is the distance from the second resonator to the detector screen, and  $T_p$  is the time it takes for the electron bunch to pass through the gap.

## PARTICLE-TRACKING SIMULATION RESULTS

Particle tracking simulations are conducted to showcase the evolution of the electron bunch, utilizing the parameters of the HUST-UED beamline [10-12], as shown in Table 3. To achieve longitudinal focusing of the electron beam within 0.45 m, as per the current design parameters of HUST-UED, a peak field of 1141 MV/m is required for the buncher. Considering the field enhancement factor, the driving THz pulse must have an energy of approximately 0.14 mJ. For the slit, the peak field is designed to be 500 MV/m, and the driving THz pulse should have an energy of about 6  $\mu\text{J}$ . Before the electron beam undergoes

streaking through the slit, it first passes through a vertical aperture with a size of 30  $\mu\text{m}$  to minimize the impact of non-uniformity in the transverse field enhancement factor of the slit on the measurement results.

Table 3: Simulation Parameters

Parameters	Value
Initial bunch length	15 fs
Bunch kinetic energy	3 MeV
Bunch charge	5 fC
Peak THz buncher field	1141 MV/m
Peak THz slit field	500 MV/m

Figure 6 (a) illustrates the imprinting of the bunch after undergoing compression and streaking, which has an initial length of 15 fs. For comparison purposes, the uncompressed bunch imprinting is also shown in Fig. 6(b). The results clearly indicate that the beam is compressed from its original duration of 54 fs to an impressive 4 fs, resulting in a compression ratio of 13. By incorporating the buncher, the temporal resolution of UED can be effectively reduced to approximately 30 fs.

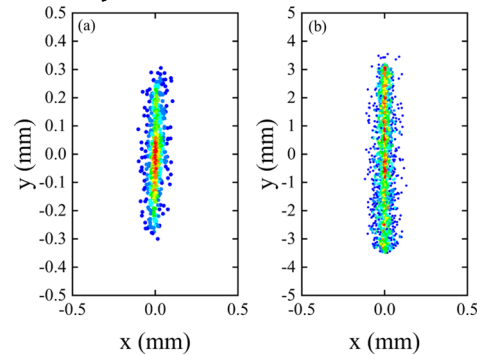


Figure 6: Comparison of bunch imprints for compressed (a) and uncompressed (b).

## CONCLUSION

In summary, the presented approach demonstrates an innovative path towards all-optical bunch length compression and measurement of electron bunches. This method ensures inherent synchronization and eliminates timing jitter, making it ideal for precise electron bunch manipulation and high-resolution diagnostics. The preliminary results demonstrate the successful compression of the electron bunch from 53 fs to 4 fs, which significantly improves the overall time resolution of UED to below 30 fs. The preliminary results highlight the potential of this proposed technique in advancing electron bunch manipulation and achieving ultra-high temporal resolution in applications involving electron-laser-related.

## ACKNOWLEDGEMENTS

The work is supported by the National Natural Science Foundation of China (NSFC 12235005), and the State Grid Corporation of China Technology Project (5400-202199556A-0-5-ZN).

## REFERENCES

- [1] R. J. Dwayne Miller, “Femtosecond Crystallography with Ultrabright Electrons and X-rays: Capturing Chemistry in Action”, *Science*, vol. 343, p. 1108-1116, 2014. doi:10.1126/science.1248488
- [2] G. Sciaini and R. J. Dwayne Miller, “Femtosecond electron diffraction: heralding the era of atomically resolved dynamics”, *Reports on Progress in Physics*, vol. 74, p. 096101, 2011. doi: 10.1088/0034-4885/74/9/096101
- [3] I. Grguraš, A. R. Maier, C. Behrens, et al., “Ultrafast X-ray pulse characterization at free-electron lasers”, *Nature Photonics*, vol. 6, p. 852-857, 2012. doi: 10.1038/nphoton.2012.276
- [4] J. Maxson, et al., “Direct Measurement of Sub-10 fs Relativistic Electron Beams with Ultralow Emittance”, *Phys. Rev. Lett.*, vol. 118, p. 154802, 2017. doi: 10.1103/PhysRevLett.118.154802
- [5] L. Zhao, et al., “Terahertz Streaking of Few-Femtosecond Relativistic Electron Beams”, *Physical Review X*, vol. 8, p. 021061, 2018. doi: 10.1103/PhysRevX.8.021061
- [6] J. Fabiańska, et al., “Split ring resonator based THz-driven electron streak camera featuring femtosecond resolution”, *Scientific Reports*, vol. 4, p. 5645, 2014. doi: 10.1038/srep05645
- [7] C. Kealhofer, et al., “All-optical control and metrology of electron pulses”, *Science*, vol. 352 p. 429-433, 2016. doi: 10.1126/science.aae0003
- [8] E. C. Snively, et al., “Femtosecond Compression Dynamics and Timing Jitter Suppression in a THz-driven Electron Bunch Compressor”, *Phys. Rev. Lett.*, vol. 124, P. 054801, 2020. doi: 10.1103/PhysRevLett.124.054801
- [9] D. Zhang, et al., “Segmented terahertz electron accelerator and manipulator (STEAM)”, *Nat. Photonics*, vol. 12, p. 336-342, 2018. doi: 10.1038/s41566-018-0138-z
- [10] Y. Xu, et al., “Towards precise diagnosis time profile of ultrafast electron bunch trains using orthogonal terahertz streak camera”, *Opt. Express*, vol. 31, p. 19777-19793, 2023. doi: 10.1364/OE.488132
- [11] C.-Y. Tsai et al., “Low-energy high-brightness electron beam dynamics based on slice beam matrix method”, *Nucl. Instrum. Methods. Phys. Res. A*, vol 937, pp. 1-20, Sep. 2019. doi:10.1016/j.nima.2019.05.035
- [12] C.-Y. Tsai and K. Fan. “A Semi-Analytical Approach to Six-Dimensional Path-Dependent Transport Matrices With Application to High-Brightness Charged-Particle Beam Transport”, in *Proc. 2019 North American Particle Acc. Conf. (NAPAC2019)*, Lansing, MI, US, Sep. 2019, pp. 792-795. doi:10.18429/JACoW-NAPAC2019-WEPLS12